Received 27 May 2022; revised 22 July 2022; accepted 8 August 2022.
Date of publication 11 August 2022; date of current version 30 August 2022.

Digital Object Identifier 10.1109/OJUFFC.2022.3198390

Assessing the Microfabrication-Related Variability of the Performance of CMUT Arrays

MONICA LA MURA [1] (Member, IEEE), ALVISE BAGOLINI [2], PATRIZIA LAMBERTI [1] (Member, IEEE), AND ALESSANDRO STUART SAVOIA [3] (Member, IEEE)

[1]Department of Information and Electrical Engineering and Applied Mathematics, University of Salerno, 84084 Fisciano, Salerno, Italy
[2]Micro Nano Facility (MNF), Bruno Kessler Foundation, 38123 Povo, Trento, Italy
[3]Department of Industrial, Electrical and Mechanical Engineering, Roma Tre University, 00146 Roma, Italy

CORRESPONDING AUTHOR: M. LA MURA (mlamura@unisa.it)

This work was supported in part by the POSITION-II Project funded by the Electronic Component and Systems for European Leadership (ECSEL) Joint Undertaking (JU) under grant number Ecsel-783132-Position-II-2017-IA, in part by the Fondi di Ateneo per la Ricerca di Base (FARB) Funds from the University of Salerno, and in part by the European Union's Horizon 2020 Research and Innovation programme under Grant agreement 881603.

ABSTRACT This paper addresses the assessment of the variability of CMUT arrays' electro-mechanical and acoustic performance, as related to the tolerance of the CMUT vertical dimensions due to the microfabrication process. A 3-factors 3-levels factorial sensitivity analysis is carried out to compute the main effects and the interaction effects of the moving plate thickness, the passivation layers thickness, and the sacrificial layer thickness, on the CMUT resonance frequency, collapse voltage, and static capacitance, as well as on the transmission and reception sensitivity amplitude and bandwidth and time delay in water-coupled condition. The analysis is performed by means of FEM simulations of the CMUT static behavior and dynamic response, and the findings are compared to experimental data.

INDEX TERMS CMUT, design of experiments, full factorial analysis, MEMS, microfabrication, reliability, robustness.

I. INTRODUCTION

THE ADVANCEMENTS in the accuracy and reliability of Silicon micromachining technology have enabled the development of high-performing MEMS devices for a growing range of applications, with the appealing characteristic of allowing the integration with CMOS-based circuits. Thanks to a decade of rapid progress, Capacitive Micromachined Ultrasonic Transducer (CMUT) technology has matured to the point of leading several companies to commercialize CMUTs for many applications in both medical imaging and airborne ultrasound.

When large-scale production is reached, a significant challenge to be addressed is the reproducibility of the fabricated device, which is highly dependent on the reliability of the manufacturing process. The two main technologies employed for the fabrication of CMUTs are sacrificial release and wafer-bonding processes. The sacrificial release was the first process used for the development of CMUT devices [1], [2], and has since been used by many due to its good reliability [3], [4], [5], [6], [7], [8]. Besides conventional bottom-to-top fabrication approaches, also a ''reverse'' fabrication process based on sacrificial release techniques has been proposed [9], [10], [11], [12], building the device with a top-to-bottom approach. These well-established technologies are based on surface micromachining techniques that create the cavity under the free-standing structure, i.e., the vibrating plate, by means of selective etching of a sacrificial layer. Typical wafer bonding methods are based on bulk micromachining and Silicon-on-Insulator (SOI) technologies [13], [14], [15], [16], [17], [18], [19], [20], [21], and consist of shaping the cavities on a Silicon wafer and then bonding the SOI wafer to form the CMUT cells. Adhesion between the bonded wafers is crucial for achieving a good yield [22]. In both CMUT fabrication approaches, the accuracy with which the different layers of the electrostatic cells are realized determines the uniformity of the transducer performance.

In the case the vibrating plate is achieved by deposition, rather than by bonding or release, its thickness has been reported to be the main parameter affecting the CMUT resonance frequency and the electrostatic behavior [16], [23], [24]. In other cases, when the plate thickness tolerance is very small, the homogeneity of the electro-mechanical response of the device is mainly determined by the uniformity of the effective gap, i.e., the multiple layers between the top and bottom electrodes [18], [23], [25].

Up to now, the uniformity of the CMUT array performance has always been evaluated in terms of standard deviation of the biased transducer resonance frequency [26], [27], [28], [29], and occasionally in terms of acoustic performance variability (e.g., sensitivity bandwidth and center frequency standard deviation) [12], [30], [31], [32]. Nevertheless, a quantitative evaluation of the effect of the fabrication-related variability of the geometrical parameters on the transducer performance variation has never been performed.

Due to the high cost in terms of resources and time of performing repeated experiments in microfabrication processes, and thanks to the good reliability of several accurate models for the CMUT electro-mechanical and electro-acoustic behavior investigation, it is possible to quantify the dependence of the performance upon the process parameters by means of designed simulations rather than experiments. This also permits to exclude the effects of unpredictable phenomena occurring throughout the experiment. For this purpose, this work relies on a well-established Finite Element Method (FEM)-based model for wide-aperture CMUT transducers with a spatially periodic layout [33]. Finite element analysis enables the assessment of the electro-acoustic response of individual cells or elements of the transducer, which would cause several measurement issues if approached by experiments.

This work follows the study presented in [34] and investigates the impact of the microfabrication-related variability of the CMUT cells vertical dimensions on the electro-mechanical and electro-acoustic performance of the finished device, assessing the sensitivity of selected quantities to the process-dependent uncertainty. The proposed sensitivity analysis is carried out by referring to a reverse-fabricated 256-element CMUT linear array for medical imaging [35]. The variability of the considered output quantities computed by the simulations is compared to the one experimentally observed for the reference device.

Section II describes the approach proposed for the analysis of the sensitivity of CMUT arrays to the design parameters variation within a small range around the nominal design, based on a three-levels factorial design of experiments. Section III reports the results of the mechanical, electro-mechanical, and electro-acoustic response variation caused by the selected geometry-related factors variation. The main findings of the proposed study are discussed in Section IV. Finally, the appendix reports the expressions for the computation of the examined quantities and their understanding.

TABLE 1. Design parameters of the reference CMUT.

Symbol	Nominal value	Mean value	Std. Dev.	Description
		Lateral dimensions (μm)		
d_m	50		0.5	LPCVD-SiN front plate diameter
p_m	57.7			Cell pitch (center-to-center distance)
d_e	34		0.5	Aluminum electrode diameter
		Vertical dimensions (nm)		
t_{mem}	2000			LPCVD-SiN front plate thickness
t_{comp}	360	359.2	1.6	PECVD- SiN compensation nitride
$t_{e,\text{top}}$	300	306	4	Al top electrode thickness
$t_{p,\text{top}}$	336	336.2	2	PECVD- SiN top passivation layer thickness
t_c	200	199	2	Sacrificial layer thickness (cavity height)
$t_{p,\text{bottom}}$	350	350.4	7.4	PECVD-SiN bottom passivation layer thickness
$t_{e,\text{bottom}}$	300			Al bottom electrode thickness
t_b	4500 *(tot)*	489.6 *(1^{st} layer)*	0.7	PECVD-SiN back passivation layer thickness

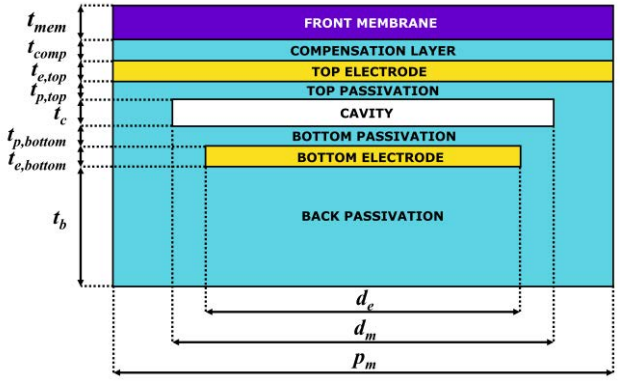

FIGURE 1. Cross section of the CMUT circular cell (not to scale).

II. MATERIALS AND METHODS

A. THE REFERENCE CMUT ARRAY

The reference device is a 256-element reverse-fabricated CMUT linear array, with an inter-element pitch of 0.2 mm and an elevation of 5.0 mm, designed for medical imaging applications. The cell, element, and array lateral dimensions are representative of CMUT linear arrays designed for medical imaging in the same frequency range. Each element is composed of $N = 344$ circular cells uniformly arranged by hexagonal tiling. Table 1 reports the nominal design parameters for the CMUT cell of the considered device and the mean and standard deviation of the vertical dimensions as obtained from in-line inspection during fabrication. The thickness data for dielectric layers are measured by interferometry on standard testing wafers in 5 predefined points. The residual stress of the dielectric layers, deposited by mixed-frequency plasma-enhanced chemical vapor deposition (PECVD), is very low (−40 MPa) [36], and the residual stress of the front-plate nitride is <100 MPa. The thickness data of the aluminum layers are measured with optical

profilometry using dedicated features on process wafers. 5 predefined points were measured on the wafer. The listed parameters are indicated in the cell cross-section shown in Fig. 1.

B. A FACTORIAL APPROACH TO THE SENSITIVITY ANALYSIS

To investigate the effect of the variation of design parameters on given quantities, several techniques can be used. Frequently, the sensitivity of the quantities of interest is assessed by varying one input factor at a time within their possible variation range identified. Though, this approach neglects the possibility that the simultaneous variation of two or more factors affects the observed output quantity differently than if the factors were varying individually. It is therefore more adequate to use a factorial approach to the design of experiments, which considers multiple cases of combined variations of factors, since this method allows the assessment of interactions between factors and a straightforward extraction of prediction models for the response variability [37], [38], [39].

1) **Choice of factors and levels**

Every geometric parameter involved in the outline of the cell structure contributes to determining the CMUT mechanical and acoustic response. However, not all parameters are characterized by the same uncertainty in the manufacturing of the device. In particular, during the microfabrication process, the lateral dimensions are better controllable than the vertical dimensions. For this reason, the uncertainty on the thickness of the plate and of the layers composing the effective gap has a greater impact on the uniformity of the device performance [40]. In this work, the sensitivity analysis was performed considering three levels of the following three factors: the moving plate thickness, sum of the thicknesses of the LPCVD SiN layer and the PECVD SiN compensation layer, $t_m = t_{mem} + t_{comp}$, the total thickness of the PECVD SiN passivation layers between the electrodes, $t_p = t_{p,top} + t_{p,bottom}$, and the sacrificial layer thickness (corresponding to the cavity height), t_c. The factors selection was conducted by considering independently the layers making up the effective gap (involved in the electro-mechanical transduction) and the mechanical part of the plate. Furthermore, the passivation layers and the sacrificial layer were also considered separately, since their thickness results from different steps of the fabrication process. In this way, the impact assessment of the accuracy of different deposition and etching steps can be more straightforward. The full factorial approach corresponds to $3^3 = 27$ possible combinations of the design parameters.

For what concerns the choice of the variation range for the design parameters, a number of technical aspects related to the thin film deposition has to be considered. The deposition chamber conditioning, the thermal contact between the wafer and chuck, and the designed tolerances of the flow meters and temperature control system will affect the deposition rate, and therefore the final thickness. A reasonable maximum value of $\pm 10\%$ variation around the nominal value was considered for each of the chosen factors. Table 2 summarizes the factors and levels of the performed tolerance analysis. Concerning the experimentally observed unevenness of the vertical dimensions, by assuming a normal distribution of the uncertainty, the bilateral variation range of each factor can be considered spanning across six times the standard deviation, centered at the mean value of each measured parameter (see Table 1). As can be noticed, the variation ranges of the factors considered in the simulations are greater than those observed in the fabricated devices. In this way, it is expected that the measured variation of the performance indicators is smaller than that obtained by the simulations. Fig. 2 shows the combinations of the factors, as obtained following the 3^3 full factorial design, in form of points located in the design parameters space. Inscribed in the cube outlined by the vertex values of the factors, the measured variation range of the factors can be seen.

TABLE 2. Input factors levels used in the simulations.

Factor	Minimum	Nominal	Maximum	$\pm\Delta$
t_m (nm)	2124	2360	2596	236
t_p (nm)	617.4	686	754.6	68.6
t_c (nm)	180	200	220	20.0
Coded	−1	0	1	

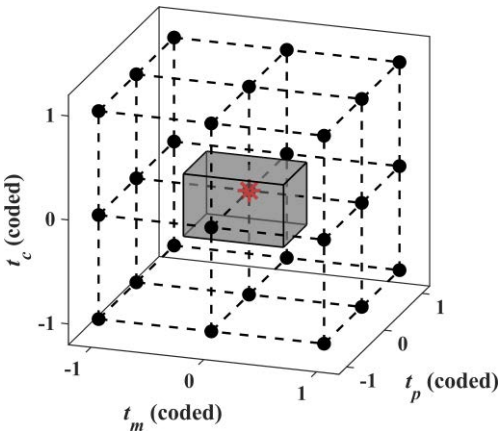

FIGURE 2. The design parameters space. According to the proposed 3^3 full factorial approach, each combination of the factor levels (here represented by the coded values −1, 0, +1) is a point in the design space. The grey box represents the measured variation of the factors, which is a subdomain of the parameters space considered in the simulations.

2) **Choice of response variables**

The quantities typically used to describe the electro-mechanical and electro-acoustic performance of a CMUT array are the unbiased and biased transducer air-coupled resonance frequency, and the water-coupled transmission (TX) and reception (RX)

TABLE 3. Selected performance indicators.

Symbol	Quantity
	Electromechanical response variables
V_c	Collapse (pull-in) voltage
C_0	CMUT cell static capacitance
f_r	Biased transducer resonance frequency
	Electroacoustic response variables
$\|G_{tx}\|$	Transmission sensitivity amplitude
τ_{tx}	Transmission sensitivity time delay
$BW_3{}^T$	Transmission sensitivity −3dB bandwidth
$\|G_{rx}\|$	Receive sensitivity amplitude
τ_{rx}	Receive sensitivity time delay
$BW_3{}^R$	Receive sensitivity −3dB bandwidth

sensitivity gain and fractional bandwidth. The unevenness of the resonance frequency across the cells of the array elements is an important indicator of the transducer quality since it is closely related to the sensitivity center frequency. Nevertheless, several other quantities offer insight into the transducer properties, providing guidance about the device biasing, driving, and read-out interfacing.

For example, analyzing the mechanical resonance frequency in zero-bias condition provides a deeper understanding of the individual role of the geometrical design parameters in the cell resonance. Furthermore, when in biased condition, the uniformity of the collapse voltage has great importance: when the CMUT array is operated in the so-called pre-collapse region, in which the vibrating plates are biased very close to the collapse voltage, the unevenness of the pull-in voltages determined by the cell-to-cell variations may cause some membranes to collapse prematurely. Consequently, to prevent the collapse, the bias voltage is usually restricted to a "safe operating zone" below 80% of the nominal collapse voltage [41]. Improving the uniformity by increasing the microfabrication process reliability would allow increasing the bias voltage closer to the pull-in voltage (hence improving the electro-mechanical coupling factor of the transducer) with lesser risk of unexpected collapse. This improvement also benefits devices operated in collapse-mode, which are reported to be even more sensitive to the effects of process-related variations [42]. It is worth noting that, for devices fabricated by the traditional sacrificial-release process, the individual cell collapse voltage and its uniformity across the element can be affected also by the cell location with respect to the element layout, due to the eventual reduced stiffness of the outer edges [43]. In the reverse process, this additional source of variation does not intervene, since the plates are all made from the same nitride layer that covers the entire wafer.

Furthermore, the variation of the static capacitance is also of interest. The capacitance affects the read-out circuit sensitivity and dynamic performance [44]; therefore, reducing the capacitance deviation from the nominal value positively impacts the read-out electronics performance. Since it is found that the geometry variations influence the CMUT static capacitance more than bias-induced diaphragm pre-stress [45], this parameter was added to the computed figures of merit.

Considering the acoustic performance of the CMUT, the sensitivity of the transmission and reception transfer functions is analyzed in terms of gain and phase, in addition to bandwidth, to investigate the impact of process-related variations also on the amplitude as well as on the time delay of the transmitted or received signal. Due to the reciprocity of the transmit sensitivity and the short-circuit current receive sensitivity, the effects of the design parameters tolerance on both transfer functions are equivalent. For this reason, we considered the open-circuit voltage receive sensitivity, representative of the condition of transducers coupled to medium-high input impedance front-end electronics, such as the most common general purpose voltage amplifiers.

Table 3 reports the full list of the response variables analyzed to assess the electro-mechanical performance and the water-coupled acoustic performance of the reference CMUT array.

Although some of the chosen quantities can be extracted from electrical impedance measurements [46], or experimentally measured, several of these require quite complex experimental set-ups, often affected by uncertainty difficult to quantify and sensitive to parasitics. Others are difficult to evaluate separately for each element of the transducer (e.g., the acoustic performance parameters), and are therefore better investigated by means of computer simulations.

C. FEM-BASED SIMULATIONS

The computation of the selected performance indicators was done by FEM simulations by means of the 2D axisymmetric model for the simulation of a circular CMUT cell described in [33]. The 2D axisymmetric model of one single cell with replication boundary conditions coupled to a half pitch-wide fluid waveguide represents an unbounded array of circular cells radiating plane waves in the acoustic medium. The unbounded transducer model intrinsically neglects the edge effects on the array element performance; nevertheless, it provides a good representation of the element behavior due to its large aperture with respect to the pressure wavelength [47]. The parametric variation of the factors was controlled by an automatic MATLAB (©The MathWorks, Inc.) routine calling the FEM software and providing the input file with the model parameters defined according to the designed combinations.

III. SENSITIVITY ANALYSIS RESULTS

A. MECHANICAL PERFORMANCE SENSITIVITY

The dependence of the first mode mechanical resonance frequency on the three input factors variation is summarized in

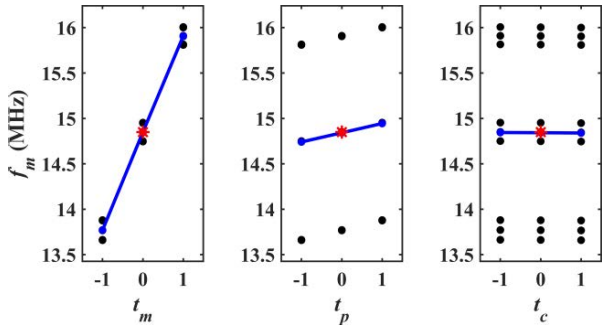

FIGURE 3. f_m data plotted against the three input factors, t_m, t_p, and t_c. The black dots represent the scattered data computed by the simulations. The red star marks the response computed in correspondence of the nominal set of input parameters. The blue lines connect the average values of the response, computed for each level of the factors.

the scatter plot shown in Fig. 3. The mechanical resonance frequency is computed by performing the finite element modal analysis of the mechanical model of the transducer in zero-bias condition. As can be seen in Fig. 3, the f_m varies linearly with the t_m and t_p, parameters, and is unaffected by the t_c variation. This behavior is in agreement with the analytical expression for the resonant frequency of a circular plate with fixed rim [48] commonly used for the fast computation of the first flexural mode resonance frequency of circular CMUT cells. Due to the linearity of the response, no interaction effects between the factors can be found.

B. ELECTRO-MECHANICAL PERFORMANCE SENSITIVITY

Fig. 4 displays the scatter plot of the electro-mechanical performance indicators, computed by FEM simulations, at the points of the design parameter space defined by the 3^3 approach and shown in Fig. 2. The average responses at each level of the factors are connected by the superimposed blue lines, to assess the linearity of the response variation. Where available, the measured response variability is represented by a grey area spanning from the minimum and maximum measured value of the output, and from the minimum and maximum value of the input factors, computed as the nominal value $\pm\, 3\sigma$.

Concerning the collapse voltage V_c, the value computed for the nominal set of the input parameters, marked by the red star in Fig. 4(a), is $V_{c,n} = 209.5$ V. From the simulations, the V_c varies between a minimum of 156.5 V and a maximum of 273 V (i.e., between -25.3% and $+30.3\%$ of its nominal value) in response to a $\pm 10\%$ variation of the considered factors. It can be noticed, in Fig. 4(a), that the V_c variation is highly linear with respect to all three factors, since the line connecting the averages is a straight line that crosses $V_{c,n}$. Further, the response is equally affected by the plate thickness and the cavity height: this result is coherent with the analytical model for the collapse voltage [49], according to which the V_c depends equally on t_m and t_c following a $t_m^{3/2}$ and $t_c^{3/2}$ relation, which is a slow varying function, therefore the V_c is highly linear in a small range of variation of

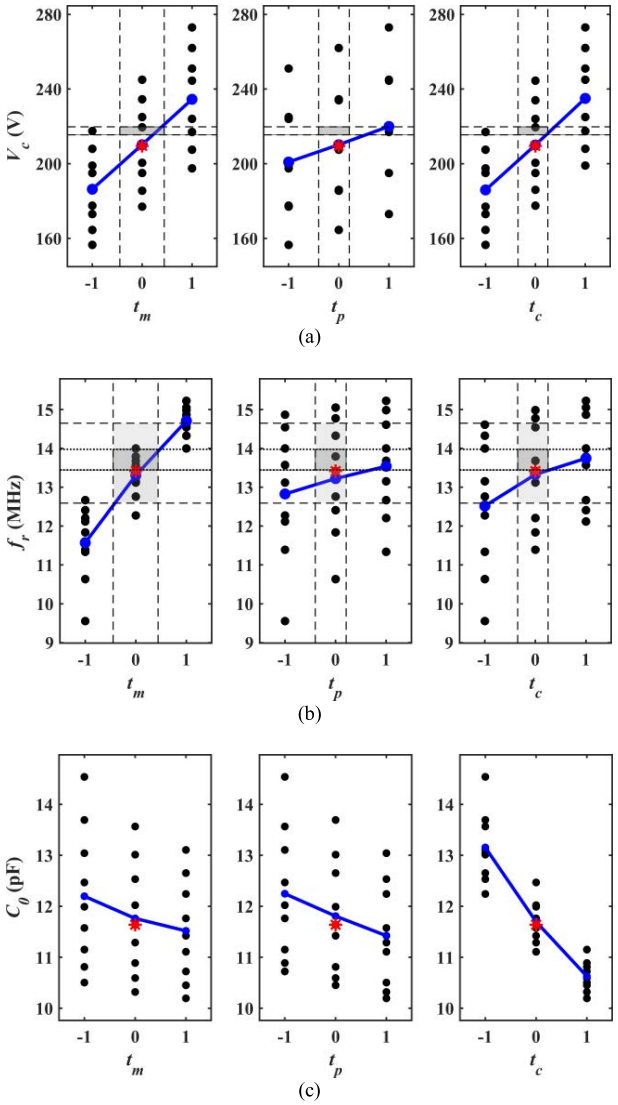

FIGURE 4. (a) V_c, (b) f_r, and (c) C_0 data plotted against the three input factors, t_m, t_p, and t_c. The black dots represent the scattered data computed by the simulations. The red star marks the response computed in correspondence of the nominal set of input parameters. The blue lines connect the average values of the response, computed for each level of the factors. The grey areas in (a) and (b) cover the surface defined by the variation range of the factors measured on one of the processed CMUT wafers, on the *x*-axis, and by the minimum and maximum value of the response measured in the CMUT characterization, on the *y*-axis. The measured response refers (a) to $N = 9$ elements of the array, and (b) to all $N = 256$ elements of the array biased at $V_{DC} = 130$ V.

the thicknesses. The measured collapse voltages are slightly higher than the nominal value obtained by the simulations, and their variability is comprised in a very small range.

The first mode resonance frequency f_r, shown in Fig. 4(b), is the result of a finite element modal analysis of the prestressed CMUT, corresponding to the electrical anti-resonance frequency of the transducer input impedance. The f_r is computed by biasing the transducer at $V_{\mathrm{DC}} = 0.7V_{c,n} = 147$ V, smaller than the lowest V_c found, to simulate a typical

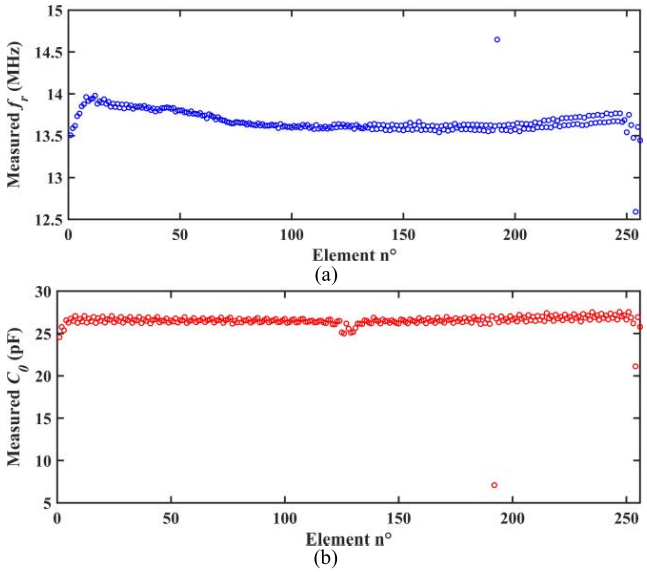

FIGURE 5. (a) The f_r, and (b) the C_0 measured by biasing the 256 elements of the reference CMUT array at V_{DC} = 130 V.

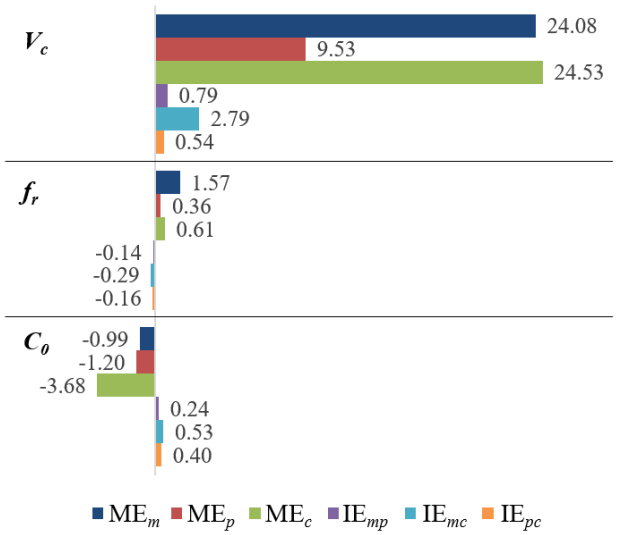

FIGURE 6. Bar chart reporting the main effects and the interaction effects for the electromechanical response quantities of interest, computed according to the 3^3 full factorial design of simulations.

biasing condition in pre-collapse operation without triggering the collapse of the plates with varied thicknesses. The resonance frequency value computed for the nominal set of the design parameters is $f_{r,\mathrm{n}} = 13.42$ MHz, and varies between 9.55 MHz and 15.22 MHz when the factors vary within a $\pm 10\%$ range. The variation of f_r is nonlinear due to the nonlinearity of the electrostatic force with respect to the distance between the electrodes and of the plate displacement with the radial position. This nonlinearity determines a non-negligible interaction effect between the factors. The measured f_r of the 256 elements of one CMUT array biased at $V_{\mathrm{DC}} = 130$ V, is reported in Fig. 5. As can be noticed, two poorly-performing elements showed a resonance frequency value very far from the nominal value and from the other measured f_r. The variation of the measured f_r is compared to the simulations in Fig. 4(b): the dashed lines enclose all the measured data between the maximum and minimum value, which are observed in correspondence of the two outliers of Fig. 5. Since the elements that showed an unexpectedly different f_r are only two, in order to make a fair assessment of the f_r variability, Fig. 4(b) also reports the maximum and minimum values of f_r measured for the other 254 elements of the array, represented by the dotted lines. In this case, the darker gray area representing the f_r variation is very narrow, confirming the robustness of the fabrication process. The measured value is generally higher than the simulated nominal value $f_{r,n}$ due to the lower bias voltage applied.

Fig. 4(c) shows the static capacitance C_0 of one element of the CMUT array, computed by biasing the transducer at $V_{\mathrm{DC}} = 147$ V. The nominal value of C_0 is $C_{0,\mathrm{n}} = 11.64$ pF, obtained by considering that the $N_c = 344$ cells of the element are electrically connected in parallel. The simulated values of C_0 range between 10.19 pF and 14.54 pF, and the capacitance is mainly affected by the sacrificial layer thickness t_c. The C_0 variation is nonlinear with the three factors, which therefore interact with each other. A direct comparison between the simulated and measured variability of the C_0 cannot be performed because the measured values of the capacitance, shown in Fig. 5(b), are strongly influenced by the parasitic capacitance due to the metal routing, both on the die and on the measurement PCB, which is not uniform between the elements.

Fig. 6 presents a summary of the main effects and interaction effects [37] computed for the considered electromechanical performance indicators, providing a direct comparison between the impact of the factors and their interactions on the different output quantities. The expressions for the main effects and interaction effects computation and their understanding are given in the Appendix. The main effects ME$_m$, ME$_p$, ME$_c$, are the coefficients representing the response location shift caused by the impact of t_m, t_p, t_c, respectively. The interaction effects IE$_{mp}$, IE$_{mc}$, IE$_{pc}$, are the coefficients accounting for the nonlinearity of the response variation caused by the interaction between the factors. As can be seen, the V_c is equally affected by the t_m and the t_c, and its variation is very linear, hence the interaction between the factors is negligible. The increase of the factors always determines an increase of the collapse voltage, because all MEs are positive. The resonance frequency unevenness is mainly due to the variations of the t_m, and the variation of f_r cannot be considered linear when the variation of the factors is $\pm 10\%$ of the nominal design value. Finally, the C_0 uniformity is mainly determined by the tolerance on the t_c. As expected, the C_0 decreases when the thickness of the plate and of the effective gap increases.

C. ACOUSTIC PERFORMANCE SENSITIVITY

The sensitivity of the acoustic performance to the process-related parameters tolerance was investigated by simulating

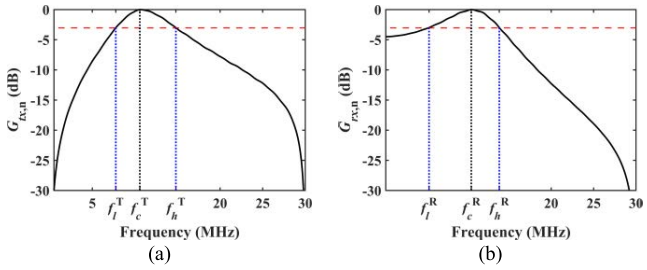

FIGURE 7. (a) The normalized Transmission Sensitivity $G_{tx,n}$ and (b) the normalized Reception Sensitivity $G_{rx,n}$, computed for the nominal set of design parameters, each reporting the low and high −3dB frequencies (in blue) and the center frequency (in black).

the CMUT in water-coupled condition and performing a pre-stressed linear harmonic analysis.

The complex transmission sensitivity transfer function, G_{tx}, was computed according to

$$G_{tx} = P_t / V_s \tag{1}$$

in which P_t is the average output pressure evaluated in the fluid at a distance of 250 μm from the radiating surface, and V_s is the input voltage provided to excite the transducer.

The complex reception sensitivity transfer function, G_{rx}, was computed according to

$$G_{rx} = V_r / P_s \tag{2}$$

in which V_r is the received voltage measured across the inner faces of the metal electrodes, and P_s is a 1 MPa pressure signal applied on the transducer's front-face in form of a load boundary condition, to simulate the effect of a pressure wave originated in the propagation fluid and impinging on the CMUT front surface. In receive mode, it is assumed that the transducer is operated in open circuit condition, as to represent the connection to a high-impedance read-out system.

The transmission sensitivity and the reception sensitivity computed for the nominal design of the considered CMUT device, $G_{tx,\mathrm{n}}$ and $G_{rx,\mathrm{n}}$, are used to obtain the nominal center frequency of both transfer functions, f_c^{T} and f_c^{R}, by

$$f_c^{\mathrm{T,R}} = (f_l^{\mathrm{T,R}} + f_h^{\mathrm{T,R}})/2 \tag{3}$$

which are used to compute the sensitivity amplitude at the nominal frequency, $|G_{tx}(j2\pi f_c^{\mathrm{T}})|$, $|G_{rx}(j2\pi f_c^{R})|$, for all the designs considered by combining the input factors. Figure 7(a) and Fig. 7(b) show the normalized $G_{tx,\mathrm{n}}$ and $G_{rx,\mathrm{n}}$, respectively, and report the nominal center frequencies f_c^{T} and f_c^{R}.

The sensitivity phase at the nominal center frequency is used to compute the time delay of the transmitted and received signal with respect to the nominal case, as defined by

$$\tau^{\mathrm{T}} = [< G_{tx,\mathrm{n}}(j2\pi f_c^{\mathrm{T}}) - < G_{tx}(j2\pi f_c^{\mathrm{T}})]/(2\pi f_c^{\mathrm{T}}) \tag{4}$$

and

$$\tau^{\mathrm{R}} = [< G_{rx,\mathrm{n}}(j2\pi f_c^{\mathrm{R}}) - < G_{rx}(j2\pi f_c^{\mathrm{R}})]/(2\pi f_c^{\mathrm{R}}) \tag{5}$$

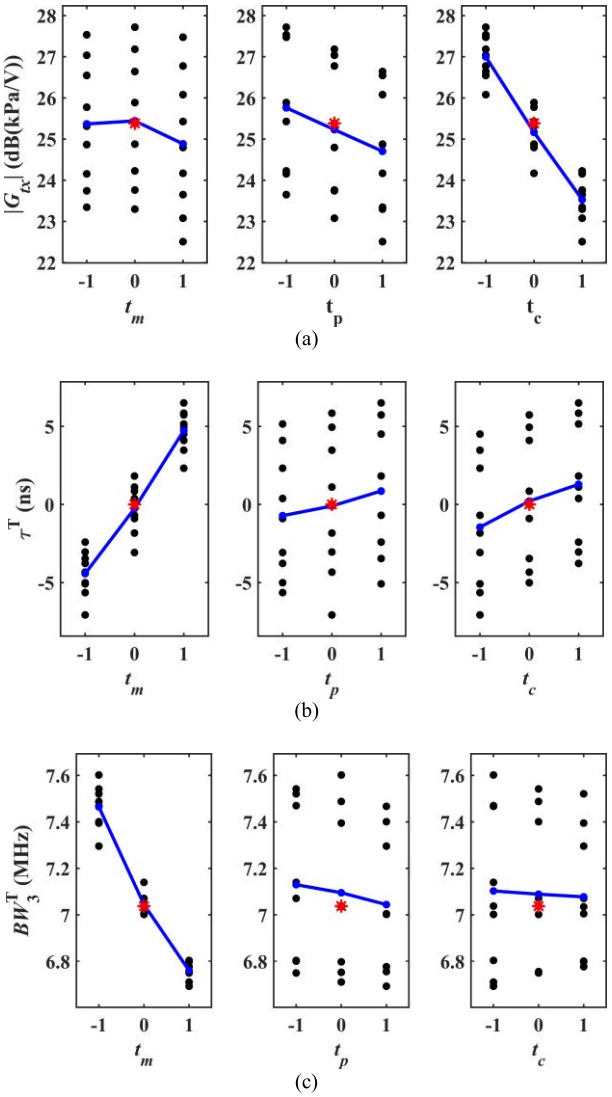

FIGURE 8. (a) $|G_{tx}|$, (b) τ^{T}, and (c) BW_3^{T} data plotted against the three input factors, t_m, t_p, and t_c. The black dots represent the scattered data computed by the simulations. The red star marks the response computed in correspondence of the nominal set of input parameters. The blue lines connect the average values of the response, computed for each level of the factors.

1) **Sensitivity of the transmission transfer function**

The amplitude, time delay, and −3dB bandwidth of the G_{tx} computed by FEM simulations of the CMUT in water-coupled condition are reported in Fig. 8(a), 8(b), and 8(c), respectively.

As shown in Fig. 8(a), the amplitude of the transmission transfer function, $|G_{tx}|$, is significantly more sensitive to the variation of the t_c. This strong influence of the t_c parameter is related to the great dependence of the electro-mechanical coupling efficiency on the distance across the electrodes. Coherently with the expectations, the increase of the t_c produces a steep decrease of the sensitivity amplitude due to the lower efficiency of the transduction from the electrical to the mechanical domain resulting from the electrodes separation.

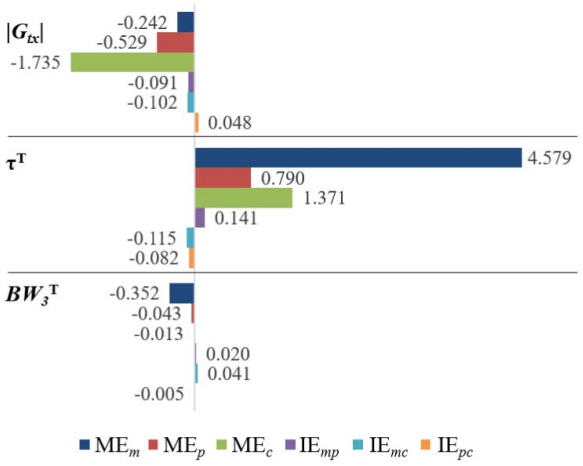

FIGURE 9. Bar chart reporting the main effects and the interaction effects for the quantities of interest of the electroacoustic response in transmit-mode, computed according to the 3^3 full factorial design of simulations.

For the $|G_{tx}|$, the t_m is the less influential factor. The variation of the three input factors of an equal percentage amount of $\pm 10\%$ results in a variation of the $|G_{tx}|$ of about $\pm 8\%$ of its nominal value $|G_{tx}|_n = 14.85$ dB(kPa/V).

The transmit-mode time delay τ^T shown in Fig. 8(b) ranges from a minimum of -7.07 ns to a maximum of $+6.50$ ns, thus the transmission of the same pulse occurs in a time window of $\Delta\tau^T = 13.57$ ns. The considered equal percentage variation of the three input factors determines a greater impact of the t_m. Generally, the increase of all thicknesses determines an increase of the delay, since the effects are all of positive sign.

Finally, the –3 dB bandwidth of the G_{tx}, BW_3^T, is shown in Fig. 8(c). The most influential parameter is the t_m, whose main effect is one order of magnitude higher than the others and is negative, i.e., the BW_3^T strongly decreases by the increasing the t_m. This behavior follows the increase of the lower cut-off frequency produced by the higher flexural stiffness of thicker plates. It can be noticed that the bandwidth variation is not only nonlinear, but also non monotone with respect to the variation of t_p and t_c. This makes it impossible to represent the variation using a first-order polynomial model with interactions.

Fig. 9 reports a synthetic overview of the main effects and the interaction effects computed for the transmit-mode parameters of interest.

2) **Sensitivity of the reception transfer function**

Fig. 10 shows the simulation results of the amplitude, time delay, and -3dB bandwidth of the G_{rx} obtained in open circuit receive-mode.

In Fig. 10(a) it can be seen that, contrarily to the $|G_{tx}|$, the most influent factor on the receive sensitivity amplitude $|G_{rx}|$ is the moving plate thickness t_m. The dependence of the $|G_{rx}|$ upon all three factors is negative,

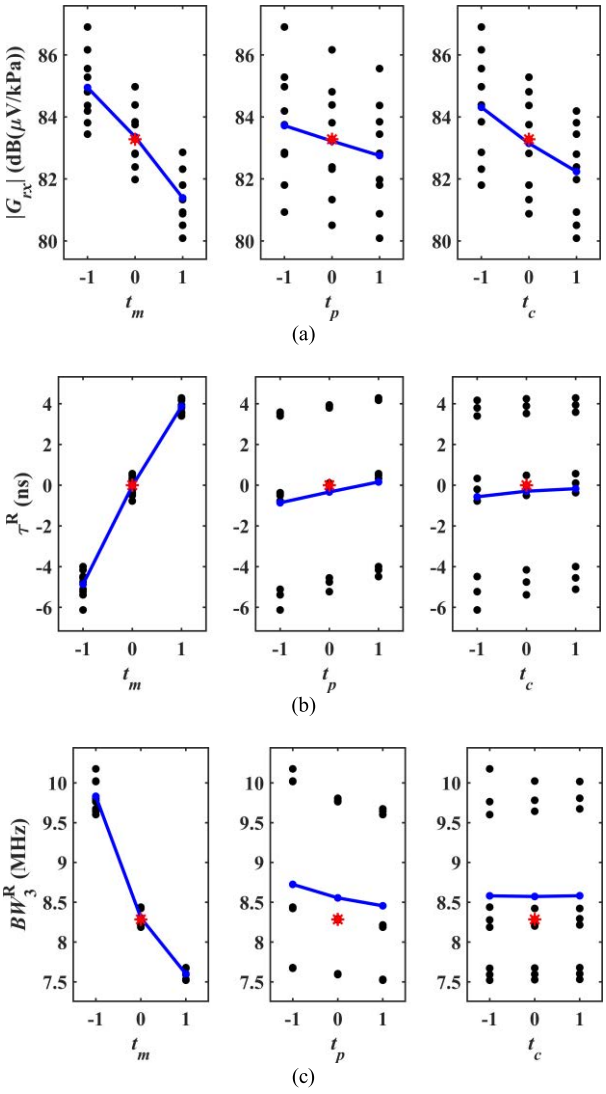

FIGURE 10. (a) $|G_{rx}|$, (b) τ^R, and (c) BW_3^R data plotted against the three input factors, t_m, t_p, and t_c. The black dots represent the scattered data computed by the simulations. The red star marks the response computed in correspondence of the nominal set of input parameters. The blue lines connect the average values of the response, computed for each level of the factors.

thus, any increase of the considered thicknesses determines a reduction of the receive sensitivity amplitude computed at the nominal center frequency. The increase of t_m and t_p corresponds to an increase of the vibrating plate thickness, thus to an increase of its flexural rigidity. The increment of the plate stiffness raises the collapse voltage, lowers consequently the normalized bias (because the applied voltage is kept constant), and therefore lessens the sensitivity. The reduction of the sensitivity amplitude produced by the increase of t_c is, also in this case, linked to the separation of the electrodes, that lowers the electro-mechanical conversion efficiency. The interaction effects are negligible with respect to the main effects, because the $|G_{rx}|$ variation has good linearity across the considered variation range

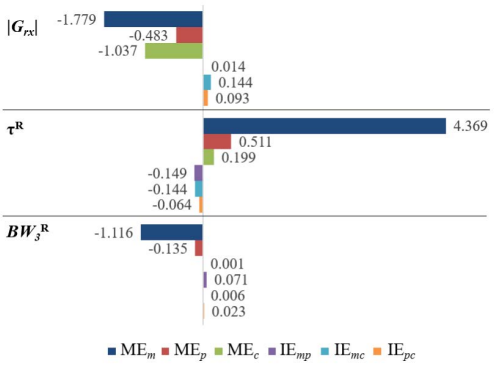

FIGURE 11. Bar chart reporting the main effects and the interaction effects for the quantities of interest of the electroacoustic response in receive-mode, computed according to the 3^3 full factorial design of simulations.

of the factors. The receive sensitivity amplitude value obtained for the nominal design at the nominal center frequency is $|G_{rx}|_{\rm n} = 83.28$ dB(μV/kPa).

For what concerns the time delay of the receive sensitivity, $\tau^{\rm R}$, Fig. 10(b) shows that t_m is by far the most effective parameter. The impact of the other two factors is negligible if compared to the effect of t_m. The results obtained for the $\tau^{\rm R}$ are very similar to those already observed for the $\tau^{\rm T}$.

The considered variation of the design parameters affects the receive sensitivity −3dB bandwidth, as shown in Fig. 10(c). The parameter that determines the greater variation of $BW_3^{\rm R}$, from the nominal value ${BW_3}^{\rm R}{}_{\rm n} = 8.285$ MHz, in response to an equal percentage variation of the input factors, is t_m. As already discussed for the transmission sensitivity case, the bandwidth reduction is caused by the increase of the plate stiffness that narrows the spread of the transfer function resonance peak. On the contrary, the cavity height t_c has the smallest impact on the bandwidth.

Figure 11 reports the main effects and the interaction effects computed for the receive-mode response.

IV. CONCLUSION

This paper proposed the assessment of the variability of the electro-mechanical and acoustic properties of CMUT arrays in response to the variation of the vertical geometrical design parameters within a given tolerance range, related to the uncontrollable uncertainty of the microfabrication process. The robustness of electro-mechanical and acoustic parameters of interest for the evaluation of the CMUT array performance was assessed by approaching the sensitivity computation by means of a design of experiments-based extreme value analysis.

The finite element analysis of the electro-mechanical and acoustic behavior of the device was compared to the experimental data obtained by the characterization of a 256-element reverse fabricated CMUT array for medical imaging. The design parameters tolerance of the considered fabrication process was measured during in-line inspection of one of the processed wafers.

Concerning the electro-mechanical parameters, it was found that the unevenness of the resonance frequency of the biased transducer is mainly ruled by the tolerance of the transducer's vibrating plate thickness, whereas the static capacitance is mainly affected by the thickness of the sacrificial layer. For what concerns the acoustic behavior of the CMUT array, it can be concluded that the sensitivity in transmission operation depends in the first place on the cavity height, and the sensitivity in reception operation is affected by all the three considered factors in a non-negligible way. Finally, the time delay and sensitivity bandwidth in both transmit and receive modes are primarily influenced by the uncertainty of the plate thickness.

This analysis provides insight into the impact of process-related tolerances on the final performance of CMUT arrays, giving directions in the investment of resources to improve any step of the microfabrication.

APPENDIX

Let us consider a n^k design of experiments, in which k input factors are divided into n levels, i.e. the i-th factor x_i with $i = 1,\ldots,k$ spreads from its minimum value, x_i^L, to its maximum value, x_i^U, by assuming n settings coded according to the relation

$$x_{i,c} = \frac{x_i - \frac{x_i^U + x_i^L}{2}}{\frac{x_i^U - x_i^L}{2}} \tag{A1}$$

(hence, $x_{i,c} = -1$ when $x_i = x_i^L$ and $x_{i,c} = +1$ when $x_i = x_i^U$).

The computation of the main effects and interaction effects is performed as follows [37].

The main effect of x_i on the performance y, ME_{x_i}, is

$$ME_{x_i} = \frac{\bar{y}_{x_i^U} - \bar{y}_{x_i^L}}{2} \tag{A2}$$

in which $\bar{y}_{x_i^U}$ and $\bar{y}_{x_i^L}$ are the average values of the considered performance computed in correspondence of the extreme values of the i-th factor settings x_i^L and x_i^U, respectively. The main effect coefficient provides a quantitative measure of the impact of x_i on y, because it represents the location shift of the average response produced by the variation of the factor between the extremes of the interval considered. The factor generating the highest change in the response, i.e. having the highest main effect, is the most influential one. Comparing the main effects of the k factors on the performance y allows ranking the input parameters according to their impact on the considered output quantity, thus distinguishing the most influential from the negligible ones.

Sometimes, the response change observed varying the factor x_j is not the same at all the settings of the factor x_i, and vice versa. This means that there is an interaction between the two factors. The computation of the interaction coefficients is

a way to quantify interactions between the input parameters impacting on the performance.

The interaction effect between the factors x_i, x_j, with $i, j = 1,\ldots, k$ and $i \neq j$, $IE_{x_i x_j}$, is

$$IE_{x_i x_j} = \frac{\left(\bar{y}_{x_i^U x_j^U} + \bar{y}_{x_i^L x_j^L}\right) - \left(\bar{y}_{x_i^U x_j^L} + \bar{y}_{x_i^L x_j^U}\right)}{2} \quad \text{(A3)}$$

and quantifies to what extent the setting of one factor impacts on the performance variation generated by the change of the other factor. In other words, it is a measure of the nonlinearity introduced in the dependence of the performance upon one factor because of its interrelation with another factor.

REFERENCES

[1] M. I. Haller and B. T. Khuri-Yakub, "A surface micromachined electrostatic ultrasonic air transducer," *IEEE Trans. Ultrason., Ferroelectr., Freq. Control*, vol. 43, no. 1, pp. 1241–1244, Jan. 1996.

[2] X. Jin, I. Ladabaum, and B. T. Khuri-Yakub, "The microfabrication of capacitive ultrasonic transducers," *J. Microelectromech. Syst.*, vol. 7, no. 3, pp. 295–302, 1998.

[3] B. Belgacem, D. Alquier, P. Muralt, J. Baborowski, S. Lucas, and R. Jerisian, "Optimization of the fabrication of sealed capacitive transducers using surface micromachining," *J. Micromech. Microeng.*, vol. 14, no. 2, p. 299, Nov. 2003.

[4] J. Knight, J. McLean, and F. L. Degertekin, "Low temperature fabrication of immersion capacitive micromachined ultrasonic transducers on silicon and dielectric substrates," *IEEE Trans. Ultrason., Ferroelectr., Freq. Control*, vol. 51, no. 10, pp. 1324–1333, Oct. 2004.

[5] Q. Zhang, P.-V. Cicek, K. Allidina, F. Nabki, and M. N. El-Gamal, "Surface-micromachined CMUT using low-temperature deposited silicon carbide membranes for above-IC integration," *J. Microelectromech. Syst.*, vol. 23, no. 2, pp. 482–493, Apr. 2014.

[6] E. Bahette, J. F. Michaud, D. Certon, D. Gross, and D. Alquier, "Progresses in cMUT device fabrication using low temperature processes," *J. Micromech. Microeng.*, vol. 24, no. 4, 2014, Art. no. 045020.

[7] A. Pirouz and F. L. Degertekin, "Low temperature CMUT fabrication process with dielectric lift-off membrane support for improved reliability," *J. Micromech. Microeng.*, vol. 28, no. 8, May 2018, Art. no. 085006.

[8] O. J. Adelegan, Z. A. Coutant, X. Zhang, F. Y. Yamaner, and O. Oralkan, "Fabrication of 2D capacitive micromachined ultrasonic transducer (CMUT) arrays on insulating substrates with through-wafer interconnects using sacrificial release process," *J. Microelectromech. Syst.*, vol. 29, no. 4, pp. 553–561, Aug. 2020.

[9] G. Caliano *et al.*, "Capacitive micromachined ultrasonic transducer (cMUT) made by a novel 'reverse fabrication process,"' in *Proc. IEEE Ultrason. Symp.*, vol. 1, Sep. 2005, pp. 479–482.

[10] A. Coppa, E. Cianci, V. Foglietti, G. Caliano, and M. Pappalardo, "Building CMUTs for imaging applications from top to bottom," *Microelectron. Eng.*, vol. 84, nos. 5–8, pp. 1312–1315, May 2007.

[11] A. Savoia, G. Caliano, B. Mauti, and M. Pappalardo, "Performance optimization of a high frequency CMUT probe for medical imaging," in *Proc. IEEE Int. Ultrason. Symp.*, Oct. 2011, pp. 600–603.

[12] A. S. Savoia, G. Caliano, and M. Pappalardo, "A CMUT probe for medical ultrasonography: From microfabrication to system integration," *IEEE Trans. Ultrason., Ferroelectr., Freq. Control*, vol. 59, no. 6, pp. 1127–1138, Jun. 2012.

[13] Y. Huang, A. S. Ergun, E. Haeggström, M. H. Badi, and B. T. Khuri-Yakub, "Fabricating capacitive micromachined ultrasonic transducers with wafer-bonding technology," *J. Microelectromech. Syst.*, vol. 12, no. 2, pp. 128–137, Apr. 2003.

[14] K. Midtbo, A. Ronnekleiv, and D. T. Wang, "Fabrication and characterization of CMUTs realized by wafer bonding," in *Proc. IEEE Ultrason. Symp.*, Oct. 2006, pp. 934–937.

[15] A. Logan and J. T. Yeow, "Fabricating capacitive micromachined ultrasonic transducers with a novel silicon-nitride-based wafer bonding process," *IEEE Trans. Ultrason., Ferroelectr., Freq. Control*, vol. 56, no. 5, pp. 1074–1084, May 2009.

[16] Y. Tsuji, M. Kupnik, and B. T. Khuri-Yakub, "Low temperature process for CMUT fabrication with wafer bonding technique," in *Proc. IEEE Int. Ultrason. Symp.*, Oct. 2010, pp. 551–554.

[17] M. Kupnik, S. Vaithilingam, K. Torashima, I. O. Wygant, and B. T. Khuri-Yakub, "CMUT fabrication based on a thick buried oxide layer," in *Proc. IEEE Int. Ultrason. Symp.*, Oct. 2010, pp. 547–550.

[18] K. K. Park, H. Lee, M. Kupnik, and B. T. Khuri-Yakub, "Fabrication of capacitive micromachined ultrasonic transducers via local oxidation and direct wafer bonding," *J. Microelectromech. Syst.*, vol. 20, no. 1, pp. 95–103, Feb. 2011.

[19] P. Zhang, G. Fitzpatrick, T. Harrison, W. A. Moussa, and R. J. Zemp, "Double-SOI wafer-bonded CMUTs with improved electrical safety and minimal roughness of dielectric and electrode surfaces," *J. Microelectromech. Syst.*, vol. 21, no. 3, pp. 668–680, Jun. 2012.

[20] F. Y. Yamaner, X. Zhang, and Ö. Oralkan, "A three-mask process for fabricating vacuum-sealed capacitive micromachined ultrasonic transducers using anodic bonding," *IEEE Trans. Ultrason., Ferroelectr., Freq. Control*, vol. 62, no. 5, pp. 972–982, May 2015.

[21] X. Zhang, F. Y. Yamaner, and O. Oralkan, "Fabrication of vacuum-sealed capacitive micromachined ultrasonic transducers with through-glass-via interconnects using anodic bonding," *J. Microelectromech. Syst.*, vol. 26, no. 1, pp. 226–234, Feb. 2017.

[22] K. Brenner, A. Ergun, K. Firouzi, M. Rasmussen, Q. Stedman, and B. Khuri–Yakub, "Advances in capacitive micromachined ultrasonic transducers," *Micromachines*, vol. 10, no. 2, p. 152, Feb. 2019.

[23] A. S. Erguri, Y. Huang, X. Zhuang, Ö. Oralkan, G. G. Yarahoglu, and B. T. Khuri-Yakub, "Capacitive micromachined ultrasonic transducers: Fabrication technology," *IEEE Trans. Ultrason., Ferroelectr., Freq. Control*, vol. 52, no. 12, pp. 2242–2258, Dec. 2005.

[24] Z. Li, L. Zhao, Z. Jiang, P. Li, Y. Hu, and Y. Zhao, "Fabrication of CMUTs with a low temperature wafer bonding technology," in *Proc. IEEE Sensors*, Dec. 2015, pp. 1–4.

[25] J. Due-Hansen *et al.*, "Fabrication process for CMUT arrays with polysilicon electrodes, nanometre precision cavity gaps and through-silicon vias," *J. Micromech. Microeng.*, vol. 22, no. 7, Jun. 2012, Art. no. 074009.

[26] S. E. Diederichsen, F. Sandborg-Olsen, M. Engholm, A. Lei, J. A. Jenseny, and E. V. Thomsen, "Fabrication of capacitive micromachined ultrasonic transducers using a boron etch-stop method," in *Proc. IEEE Int. Ultrason. Symp. (IUS)*, Nov. 2016, pp. 1–4.

[27] F. Y. Yamaner, X. Zhang, and Ö. Oralkan, "Fabrication of anodically bonded capacitive micromachined ultrasonic transducers with vacuum-sealed cavities," in *Proc. IEEE Int. Ultrason. Symp. (IUS)*, Oct. 2014, pp. 604–607.

[28] J. Zahorian *et al.*, "Monolithic CMUT-on-CMOS integration for intravascular ultrasound applications," *IEEE Trans. Ultrason., Ferroelectr., Freq. Control*, vol. 58, no. 12, pp. 2659–2667, Dec. 2011.

[29] H. Martinussen, A. Aksnes, E. Leirset, and H. E. Engan, "CMUT characterization by interferometric and electric measurements," *IEEE Trans. Ultrason., Ferroelectr., Freq. Control*, vol. 56, no. 12, pp. 2711–2721, Dec. 2009.

[30] I. O. Wygant *et al.*, "Integration of 2D CMUT arrays with front-end electronics for volumetric ultrasound imaging," *IEEE Trans. Ultrason., Ferroelectr., Freq. Control*, vol. 55, no. 2, pp. 327–341, Feb. 2008.

[31] D.-S. Lin *et al.*, "Packaging and modular assembly of large-area and fine-pitch 2-D ultrasonic transducer arrays," *IEEE Trans. Ultrason., Ferroelectr., Freq. Control*, vol. 60, no. 7, pp. 1356–1375, Jul. 2013.

[32] G. Gurun *et al.*, "Single-chip CMUT-on-CMOS front-end system for real-time volumetric IVUS and ICE imaging," *IEEE Trans. Ultrason., Ferroelectr., Freq. Control*, vol. 61, no. 2, pp. 239–250, Feb. 2014.

[33] M. La Mura, N. A. Lamberti, B. L. Mauti, G. Caliano, and A. S. Savoia, "Acoustic reflectivity minimization in capacitive micromachined ultrasonic transducers (CMUTs)," *Ultrasonics*, vol. 73, pp. 130–139, Jan. 2017.

[34] M. La Mura, A. Bagolini, P. Lamberti, and A. S. Savoia, "Impact of the variability of microfabrication process parameters on CMUTs performance," in *Proc. IEEE Int. Ultrason. Symp. (IUS)*, Sep. 2020, pp. 1–4.

[35] P. Mattesini, A. S. Savoia, A. Ramalli, F. Quaglia, P. Tortoli, and E. Boni, "Comparative assessment of plane wave imaging with 256-element CMUT and single crystal probes," in *Proc. IEEE Int. Ultrason. Symp. (IUS)*, Sep. 2021, pp. 1–3.

[36] A. Picciotto, A. Bagolini, P. Bellutti, and M. Boscardin, "Influence of interfaces density and thermal processes on mechanical stress of PECVD silicon nitride," *Appl. Surf. Sci.*, vol. 256, no. 1, pp. 251–255, Oct. 2009.

[37] D. C. Montgomery, *Design and Analysis of Experiments*, 9th ed. Hoboken, NJ, USA: Wiley, 2017.

[38] P. Lamberti, V. Tucci, M. S. Sarto, and A. Tamburrano, "Impact of physical parameters on time-delay performances of CNT-based interconnects," in *Proc. 9th IEEE Conf. Nanotechnol. (IEEE-NANO)*, Jul. 2009, pp. 54–57.
[39] M. La Mura, P. Lamberti, and V. Tucci, "Numerical evaluation of the effect of geometric tolerances on the high-frequency performance of graphene field-effect transistors," *Nanomaterials*, vol. 11, no. 11, p. 3121, Nov. 2021.
[40] A. Bagolini *et al.*, "PECVD low stress silicon nitride analysis and optimization for the fabrication of CMUT devices," *J. Micromech. Microeng.*, vol. 25, no. 1, Dec. 2014, Art. no. 015012.
[41] B. A. Greenlay and R. J. Zemp, "Fabrication of linear array and top-orthogonal-to-bottom electrode CMUT arrays with a sacrificial release process," *IEEE Trans. Ultrason., Ferroelectr., Freq. Control*, vol. 64, no. 1, pp. 93–107, Jan. 2017.
[42] K. K. Park, Ö. Oralkan, and B. T. Khuri-Yakub, "A comparison between conventional and collapse-mode capacitive micromachined ultrasonic transducers in 10-MHz 1-D arrays," *IEEE Trans. Ultrason., Ferroelectr., Freq. Control*, vol. 60, no. 6, pp. 1245–1255, Jun. 2013.
[43] A. S. Havreland, M. Engholm, C. V. Sorensen, and E. V. Thomsen, "Pull-in analysis of CMUT elements," in *Proc. IEEE Int. Ultrason. Symp. (IUS)*, Sep. 2020, pp. 1–4.
[44] M. Sautto, A. S. Savoia, F. Quaglia, G. Caliano, and A. Mazzanti, "A comparative analysis of CMUT receiving architectures for the design optimization of integrated transceiver front ends," *IEEE Trans. Ultrason., Ferroelectr., Freq. Control*, vol. 64, no. 5, pp. 826–838, May 2017.
[45] L.-M. Faller and H. Zangl, "Considerations on pre-stress in a 3D-printed capacitive force/pressure sensor," in *Proc. 18th Int. Conf. Thermal, Mech. Multi-Phys. Simul. Exp. Microelectron. Microsyst. (EuroSimE)*, Apr. 2017, pp. 1–6.
[46] A. S. Savoia, B. Mauti, and G. Caliano, "Accurate evaluation of the electro-mechanical and parasitic parameters of CMUTs through electrical impedance characterization," in *Proc. IEEE Int. Ultrason. Symp. (IUS)*, Sep. 2017, pp. 3–6.
[47] G. G. Yaralioglu, A. S. Ergun, and B. T. Khuri-Yakub, "Finite-element analysis of capacitive micromachined ultrasonic transducers," *IEEE Trans. Ultrason., Ferroelectr., Freq. Control*, vol. 52, no. 12, pp. 2185–2198, Dec. 2005.
[48] L. E. Kinsler and A. R. Frey, *Fundamentals of Acoustics*, 4th ed. New York, NY, USA: Wiley, 2000.
[49] H. Köymen *et al.*, "An improved lumped element nonlinear circuit model for a circular CMUT cell," *IEEE Trans. Ultrason., Ferroelectr., Freq. Control*, vol. 59, no. 8, pp. 1791–1799, Aug. 2012.

MONICA LA MURA (Member, IEEE) received the B.S. and M.S. degrees *(cum laude)* in electronic engineering from the University of Salerno, Fisciano, Italy, in 2011 and 2015, respectively, and the Ph.D. degree in industrial engineering (electronics) from the University of Salerno in 2019.

Since 2019, she has been a Post-Doctoral Researcher at the Department of Information and Electrical Engineering and Applied Mathematics, University of Salerno. Her research interests include the modeling, design, and characterization of micro- and nano-electronic devices. Her activities involve the investigation, by means of multiphysics finite element models and equivalent circuit models, of micro and nano electro-mechanical transducers, of graphene-based transistors for RF applications, and of 2D materials-based metasurfaces for THz devices.

Dr. La Mura serves as a Secretary for the WIE Italy AG.

ALVISE BAGOLINI received the B.Sc. degree in physics from the University of Trento, Italy, in 2001.

He was a Researcher at ITC IRST, MEMS Group. Since 2008, he has been a MEMS Process Engineer with the Micro-Nano Fabrication Facility, Fondazione B. Kessler, Kessler Research Foundation. His main fields of activity are microfabrication technology development, device layout, and testing of mechanical properties of thin films for MEMS devices.

PATRIZIA LAMBERTI (Member, IEEE) was born in 1974. She received the Laurea degree in electronic engineering and the Ph.D. degree in information engineering from the University of Salerno, Italy, in 2001 and 2006, respectively.

Since 2005, she has been a Professor of electrical engineering with the Department of Information and Electrical Engineering and Applied Mathematics (DIEM), University of Salerno. She joined the Interdipartimental Research Center for Nanomaterials and Nanotechnology (NanoMates), University of Salerno, acting as the Vice-Dean, and the Italian Inter-University Research Center for Interaction between Electromagnetic Fields and Biosystems (ICEmB), acting as a Scientific Representative for the University of Salerno Unit. Since 2002, she has been involved in experimental and numerical research on device, materials, and innovative composites for electrical engineering applications in several fields, with emphasis on robust design in presence of uncertainty. She has authored over 110 scientific publications in international journals and in proceedings of international conferences.

Prof. Lamberti is member of the "International Society for Electroporation-Based Technologies and Treatments" (ISEBTT), taking part in its foundation in 2016, and the European Aeronautic Science Network (EASN). She has been awarded of Best Paper Award in CAS2009 Conference in 2009. She has been serving IEEE as the Vice-Chair of the IEEE Italy Women in Engineering Affinity Group since 2016.

ALESSANDRO STUART SAVOIA (Member, IEEE) received the Laurea (M.S.) and Ph.D. degrees in electronic engineering from Roma Tre University, Italy, in 2003 and 2007, respectively.

He leads research activities at the Acoustoelectronics Laboratory, Department of Industrial, Electronic, and Mechanical Engineering, Roma Tre University, in the field of ultrasonic transducers. His research interests are mainly focused on the development and system integration of MEMS ultrasonic transducers (CMUT and PMUT).

Dr. Savoia has been serving the UFFC Society as an Associate Editor for the IEEE Transactions on Ultrasonics, Ferroelectrics, and Frequency Control since 2017, the Co-Chair of the TPC Group 5 "Transducers and Transducer Materials" of the International Ultrasonics Symposium since 2018, and an Elected Member of AdCom since 2021.